

# Mixing unmixables: Unexpected formation of Li-Cs alloys at low pressure

Serge Desgreniers,<sup>1\*</sup> John S. Tse,<sup>2\*</sup> Takahiro Matsuoka,<sup>3,4</sup> Yasuo Ohishi,<sup>3</sup> Justin J. Tse<sup>5</sup>

2015 © The Authors, some rights reserved; exclusive licensee American Association for the Advancement of Science. Distributed under a Creative Commons Attribution NonCommercial License 4.0 (CC BY-NC). 10.1126/sciadv.1500669

Contrary to the empirical Miedema and Hume-Rothery rules and a recent theoretical prediction, we report experimental evidence on the formation of Li-Cs alloys at very low pressure (>0.1 GPa). We also succeeded in synthesizing a pure nonstoichiometric and ordered crystalline phase from an approximately equimolar mixture and resolved its structure using the maximum entropy method. The new alloy has a primitive cubic cell with the Li atom situated in the center and the Cs at the corners. This structure is stable to at least 10 GPa and has an anomalously high coefficient of thermal expansion at low pressure. Analysis of the valence charge density shows that electrons are donated from Cs to the Li “*p*”-orbitals, resulting in a rare formal oxidation state of  $-1$  for Li. The observation indicates the diversity in the bonding of the seeming simple group I Li element.

## INTRODUCTION

According to the time-honored empirical Miedema (1) and Hume-Rothery rules (2), if there is a large disparity in the atomic sizes and small difference in electronegativity, some binary alloys are not expected to form solid solutions under ambient conditions. An example is elemental lithium (Li) and cesium (Cs), where no Li-Cs alloy has been found to exist under ambient pressure. Pressure has been recognized to be an efficient thermodynamic parameter to modify the electron states, and the synthesis may become feasible. Highly compressed Li-Cs is a system of topical interest and has motivated several theoretical investigations. In one theoretical study, it is shown that the application of pressure can alter the repulsive nature of the nonreactive Li-Cs mixture, converting an unequivocal phase separation situation at ambient pressure to a strong long-range ordering at high pressures (>50 GPa) (3). Zhang and Zenger predicted that intermetallic crystalline structures can be stabilized as a result of a pressure-induced increase in charge transfer from Li to Cs. A more recent study also predicted that under pressure, electrons can be transferred from Li in Li-rich Li-Cs alloys, causing Cs to become anionic with a formal charge larger than  $-1$  (4). These proposals are not unreasonable because pressure-promoted electron transfer in solids is not uncommon. A good example is the formation of solid solutions of  $K_2Ag$  and  $K_3Ag$  (5). Theoretical analysis showed that the K-Ag alloys form because of the electronegativity difference resulting in electrons being transferred from K 4s to unfilled Ag 5s and 5p orbitals. As a result, the overlaps between spatially extended Ag 5p orbitals are enhanced and this helps to stabilize the alloy framework with the smaller K ions as “spectators” occupying the interstitial sites (6). With this view in mind, the proposed charge transfer from Li to Cs at high pressure is not unreasonable. The motivation for this study is to explore these hypotheses and the possible existence of novel Li-Cs alloys under pressure. We uncovered several surprising results. As demonstrated below, Li-Cs alloys can readily form at very low pressure. Notably, the structure of a nonstoichiometric crystalline Li-Cs inter-

metallic compound was resolved, and the analysis of the electron density topology revealed an unusual charge transfer from Cs to Li and forming Li anion.

## RESULTS

Mixtures of Li and Cs metals of different concentrations were examined by in situ synchrotron powder x-ray diffraction under pressure and temperature. In the first experiment, the x-ray diffraction pattern was recorded immediately after a sample loading (~1:1 volume ratio, that is, Cs-dominant given the higher density of Cs) at 1.77 GPa and room temperature, as shown in Fig. 1. Even at this very small compression, a complex x-ray diffraction pattern was observed, with Bragg reflections not belonging to elemental Cs and Li. Moreover, changes in the diffraction peak positions with pressure suggested that there was more than one phase present in the sample. As illustrated in Fig. 1, two phase transitions were also detected at 2.60 and 4.5 GPa and at room temperature in the solid mixture. The complexity and the possibility of multiple components in the recorded x-ray diffraction patterns have prevented the determination of the underpinning crystalline structures. Because the possibility of phase mixtures is not ruled out, the identification of individual x-ray diffraction patterns and structure determination require a more detailed analysis. The most significant conclusion following from this first part of our experimental study is that the formation of Li-Cs crystalline alloys does occur unambiguously in a pressure regime much lower than theoretically predicted, that is, >50 GPa (3). The observed structures are likely not related to the predicted Li-rich Cs alloys (4).

In the second set of experiments, an approximate equimolar Li and Cs mixture was prepared. This was accomplished by first computing the relative volumes appropriate to achieve this stoichiometry from the elemental densities. Then, the respective volume of metals was visually estimated and appropriately loaded in the diamond anvil cell (DAC). The x-ray diffraction pattern recorded at the initial pressure of 0.12 GPa and 298 K (Fig. 2A) indicated a mixture of body-centered cubic elemental Li and Cs. At this Li-Cs concentration, alkali metals with small and large atomic radii do not intermix to form solid solutions. However, marked changes in the x-ray diffraction patterns were observed starting at ~3 GPa, as a hint on the formation of a new crystalline phase. As shown in Fig. 2A, a much simpler x-ray diffraction

<sup>1</sup>Laboratoire de physique des solides denses, University of Ottawa, Ottawa, Ontario K1N 6N5, Canada. <sup>2</sup>Department of Physics and Engineering Physics, University of Saskatchewan, Saskatoon, Saskatchewan S7N 5B2, Canada. <sup>3</sup>Spring-8/JASRI, 1-1-1 Kouto, Sayo-cho, Sayo-gun, Hyogo 679-5198, Japan. <sup>4</sup>Department of Materials Science and Technology, Gifu University, 1-1 Yanagido, Gifu 501-1193, Japan. <sup>5</sup>Robarts Research Institute, Western University, London, Ontario N6A 5B7, Canada. \*Corresponding author. E-mail: serge.desgreniers@uottawa.ca (S.D.); john.tse@usask.ca (J.S.T.)

pattern had emerged at 4 GPa, with no further changes recorded up to 8 GPa. The x-ray diffraction pattern obtained can be indexed to a primitive cubic unit cell ( $Pm\bar{3}m$ ). The cubic cell parameter monotonously decreases from 3.585(9) Å at 3 GPa to 3.489(3) Å at 8 GPa (Fig. 2, bottom). To investigate the stability of the new alloy phase, we increased the sample temperature by resistive heating to 498 K. Starting at 8 GPa, the final pressure increased to 9.6 GPa upon heating. This resulted in no further change in the x-ray diffraction pattern (Fig. 2B). While keeping the temperature constant at 498 K, the pressure was then gradually reduced. The new crystalline structure was maintained at a pressure as low as 1.9 GPa at 498 K. At lower pressures, the x-ray diffraction pattern of the sample showed a dissociation of the alloy back to elemental Li and Cs solids. For the same sample, the x-ray diffraction pattern only revealed a single phase in the

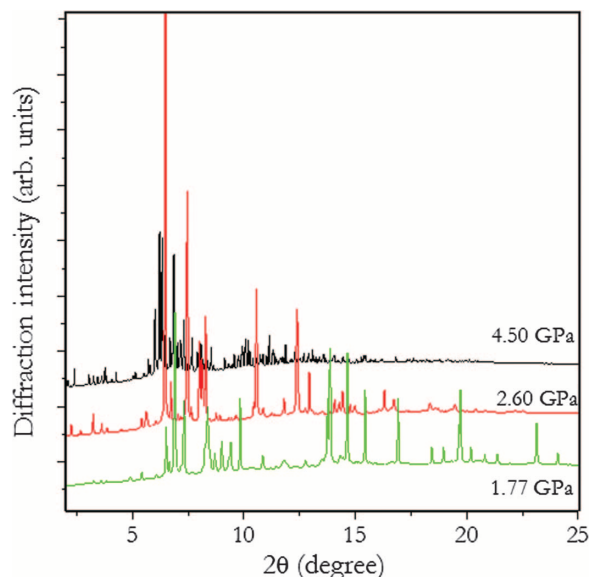


**Fig. 1. Synchrotron x-ray diffraction patterns for a starting mixture of Cs-rich Li-Cs, synthesized at low pressure and at 298 K.** Obvious changes in x-ray diffraction patterns were observed as a function of pressure. Radiation wavelength is 0.41373 Å.

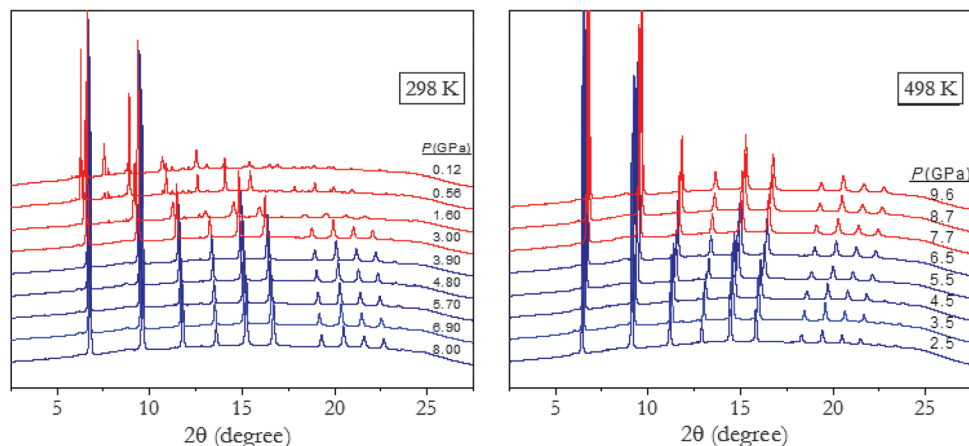


**Fig. 2. Synchrotron x-ray diffraction patterns for an approximately equimolar Li-Cs mixture at 298 K (A, left panel) and 498 K (B, right panel) at various pressures.** Note that x-ray diffraction patterns were recorded for pressure upstroke and downstroke at 298 and 498 K, respectively.

range of 3 to 10 GPa, regardless of the temperature (room or high temperature).

One striking observation was the very large coefficient of linear thermal expansion ( $\alpha$ ) of the unit cell size at 298 and 498 K (Fig. 3, top). At 3 GPa,  $\alpha$  is calculated to be  $1.7 \times 10^{-4} \text{ K}^{-1}$ , which is one order of magnitude larger than that of most solids under ambient pressure. However, as the pressure was increased, the  $\alpha$  value for the Li-Cs alloy dropped; at 8 GPa, it decreased to  $1.1 \times 10^{-4} \text{ K}^{-1}$ . The large  $\alpha$  obtained at low pressure suggests a rather weak atomic interaction (and possibly very large anharmonicity). The anomalously large  $\alpha$  is reminiscent of the fluxional dynamics observed in the “distorted simple cubic” phase of calcium for which an  $\alpha$  value of  $2.4 \times 10^{-4}$  was measured at 42 GPa (7).

Attempts to determine the atomic positions in the crystalline alloy using conventional methods were not successful in producing a reasonable structural model. The x-ray powder diffraction data, suitably well averaged and presenting minimal preferred orientation, were then analyzed using the maximum entropy method (MEM) (8). With MEM, a structural model can be obtained from the three-dimensional (3D) charge density probability distribution directly computed from the intensities of the Bragg reflections, with the space group and the lattice parameter(s) of the crystal being the only input. MEM is particularly well suited for high-pressure experiments because x-ray diffraction information is often limited and restricted to low Bragg angle reflections. Previous studies have shown that MEM is reliable in extracting (semi-) quantitative charge density distributions from powder x-ray diffraction data in dense solids at high pressure (9, 10). Moreover, although the x-ray form factor of Cs is much larger than that of Li and, consequently, the intensities of the Bragg reflections are dominated by the scattering arising from Cs atoms, MEM is able to reveal the electron density even from weak x-ray scatterers, such as hydrogen (11). We applied this method to the powder x-ray diffraction patterns obtained from the Li-Cs alloy; the resulting 3D charge density probability distribution determined at 8 GPa is depicted in Fig. 4. It is obvious that the charge densities obtained at the corner of the cubic lattice are more pronounced (larger) than what is located around the unit cell center. With this result, it is thus reasonable to assign equivalent atoms located at the corners of the cubic lattice, that is, one atom at (0,0,0) to Cs, leaving a Li situated at the  $(\frac{1}{2}, \frac{1}{2}, \frac{1}{2})$  center position

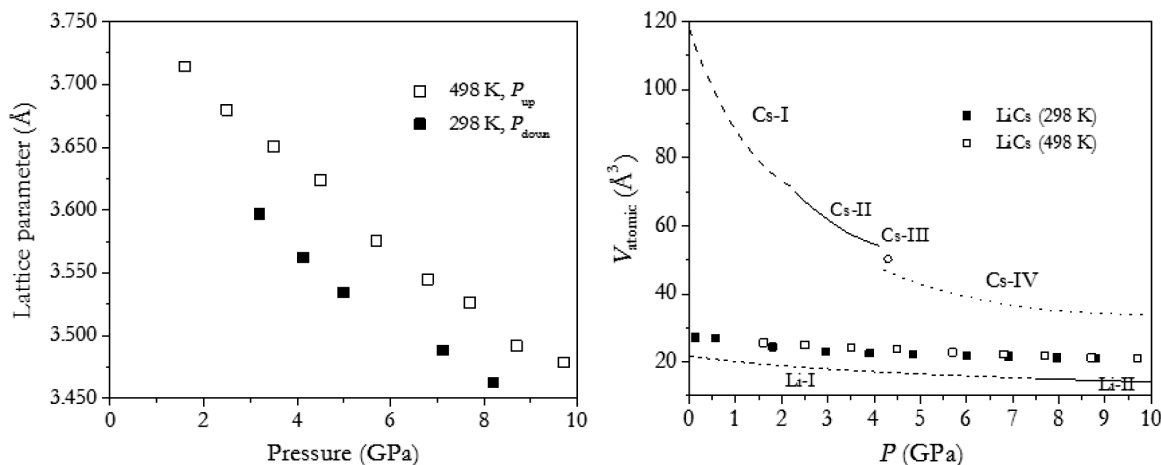


**Fig. 3. Compression of the cubic Li-Cs alloy. (Left panel)** Unit cell parameter of the cubic Li-Cs alloy at a function and pressure at two different temperatures, namely, 298 and 498 K. **(Right panel)** Comparison of the pressure dependence of the average atomic volume in Li-Cs alloys at 298 and 498 K (this work) occupied by Cs in Cs-I (14), Cs-II (15), Cs-III (17), and Cs-IV (16) and Li in Li-I (14) and Li-II (30).

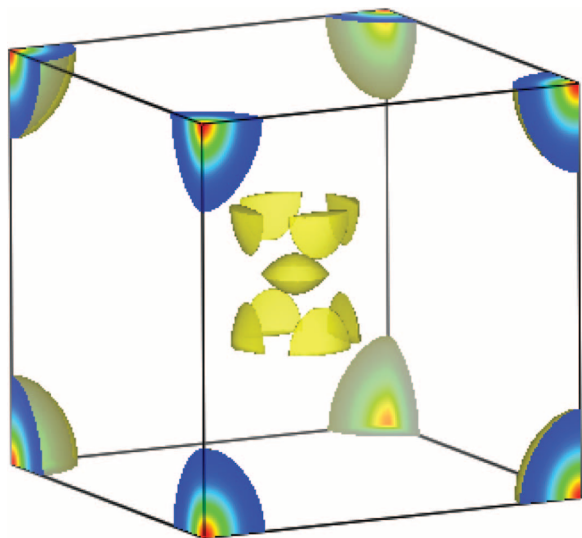


**Fig. 4. Three-dimensional electron density probability as obtained from an analysis of x-ray diffraction data by the MEM.** The x-ray data are for the Li-Cs sample at 8 GPa and 298 K. The surface contour value is  $3.25 e^-/\text{Å}^3$ .

(structural model B). The atomic site assignment was confirmed by a full pattern refinement (Rietveld) for which a substantially better fit was achieved (that is, for structural model B as opposed to model A, as illustrated in Fig. 5). For this analysis, we concluded that the alloy is an ordered solid solution of Li and Cs. Incidentally, the observed structure is similar to the stoichiometric Li-Cs B2 structure that was predicted to be stable above 100 GPa (3). This, of course, was not found to be the case. The spread of the electron density around the Li site, which correlated to the density probability distribution derived from the MEM analysis, is somewhat delocalized as compared to what is obtained around the Cs atomic sites. Although the charge density distribution derived by MEM (Fig. 4) may not be sufficiently quantitative, the Li occupancy estimated from the integrated charge density

is about 0.7; thus, the Li-Cs solid may not be perfectly stoichiometric. The structural assignment and atomic occupancies are consistent with the experimental volume of about one Cs atom per unit cell and the Cs-Cs distance of only one cell length, or  $3.585(9) \text{ Å}$  at 3 GPa.

## DISCUSSION

Under ambient conditions, elemental Cs has a body-centered cubic structure (Cs-I) (12–14). At a pressure of 2.7 GPa, it transforms to a face-centered cubic structure (Cs-II). A volume collapse was observed at a pressure of 4.5 GPa (15) because of the appearance of the tetragonal Cs-IV phase (16). Between 4.2 and 4.3 GPa, we found a complex modulated structure of phase Cs-III (17). The large volume change at 4.5 GPa is associated with the Cs  $6s \rightarrow 5d$  hybridization (18). Therefore, below 4.5 GPa, Cs is still a main group  $sp$  metal. As discussed above, the charge density topology around the Cs that results in the formation of a crystalline Li-Cs solid probably does not arise from the  $s \rightarrow d$  transition. The Cs-Cs nearest-neighbor distance in cubic Cs-II is  $4.23 \text{ Å}$  (15) and ranges from 3.7 to  $4.2 \text{ Å}$  in Cs-III (16). These Cs-Cs distances are longer than that observed in the Li-Cs alloy. Hence, the estimated average volume occupied by a Cs atom in the Li-Cs is significantly smaller than what is found in dense phases of pure Cs (Fig. 3, bottom). An explanation for the shorter nearest-neighbor contact distance found in the alloy is that the spatial extent of electron distribution around the Cs atoms is reduced as a result of a charge transfer from the  $6s$  to the Li L-shell ( $2s$  and  $2p$ ). This situation is possible because Cs is more electropositive than Li and, according to the Pauling scale, the difference in electronegativity [ $\Delta\chi = \chi(\text{Li}) - \chi(\text{Cs})$ ] is almost 0.2. The consequences of the electron transfer are that (i)  $\text{Cs}^{\delta+}$  is now smaller and  $\text{Li}^{\delta-}$  becomes larger and (ii) Cs positive ions can be brought closer together as a result of compression. This situation resembles the close contacts between  $\text{K}^+$  ions found in  $\text{K}_3\text{Ag}$  (5, 6). Thus, a shorter Cs contact distance ( $3.586 \text{ Å}$ ) in the alloy than in the elemental solid is indicative of the presence of Cs positive ions. This suggestion is supported by an inspection of the electron density topology (Fig. 4). The nearly spherical electron density around the Cs atoms indicates no noticeable electron transfer from the  $6s$  to the directional  $5d$  orbitals. In contrast, the

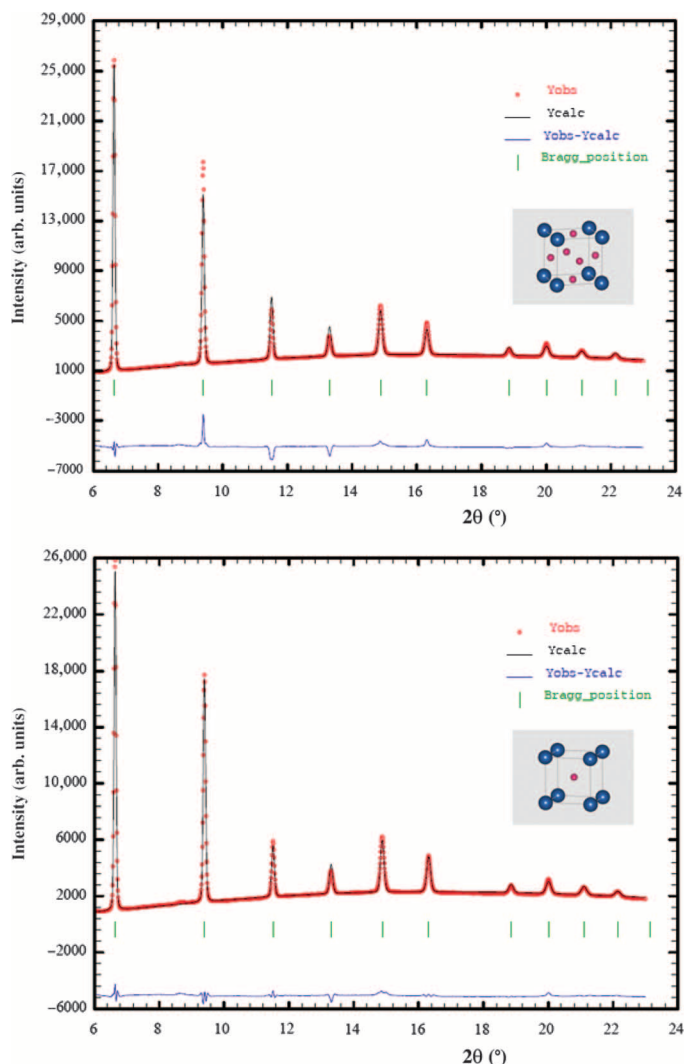


**Fig. 5. Results of a Rietveld analysis of the high-temperature/high-pressure (498 K and 5 GPa) x-ray data of the Li-Cs alloy using two different cubic structural models (symbols, observed x-ray diffraction pattern; solid black line, calculated x-ray diffraction pattern; solid blue line, intensity difference). (Top) Structural model A. Space group  $Pm\bar{3}m$ ; atomic positions: Cs (0,0,0) and Li ( $0, \frac{1}{2}, \frac{1}{2}$ ), Li ( $\frac{1}{2}, 0, \frac{1}{2}$ ), Li ( $\frac{1}{2}, \frac{1}{2}, 0$ ); lattice parameter = 3.572(4) Å;  $R_p$  = 20.1% and  $R_{wp}$  = 17.1%. (Bottom) Structural model B. Space group  $Pm\bar{3}m$ ; atomic positions Cs (0,0,0) and Li ( $\frac{1}{2}, \frac{1}{2}, \frac{1}{2}$ ); lattice parameter = 3.572(3) Å;  $R_p$  = 16.9% and  $R_{wp}$  = 9.18%.**

electron distribution at the Li shows directionality and is spatially more extended with a mean  $l$  width of  $\sim 1.7$  Å. This observation suggests that electrons are being transferred from Cs to the Li  $2s$ - $2p$  hybrid orbitals (vide supra). It is informative to compare the Li-Cs alloy found in this study with the high-pressure phase of CsF, which also bears a simple cubic structure (19) but with a smaller lattice parameter of 3.38 Å at 4.8 GPa. The lattice parameter of Li-Cs at the corresponding pressure is 3.53 Å (Fig. 3). The larger radius of a neutral Li atom (1.37 Å) compared with that of an F anion (1.19 Å)

(20) may account for the expansion of the lattice parameter. Moreover, the spatial extent of the Li anion is expected to be even larger.

Here, it is shown that, although group I Li and Cs do not combine under normal conditions, it is possible to force the two unmixable elements to readily form binary alloys at very low pressure. The Li-Cs solids unveiled represent the very first observations of binary alloys obtained from isovalent but very dissimilar alkali metals. In a way, the experimental results apparently contradict the theoretical structural prediction that Li-Cs alloys can only be obtained at significantly higher pressure, namely, above 50 GPa (3, 4). Evidently, there is no strong repulsive force between Li and Cs as they become miscible, and they easily establish a long-range order at very low compression. It should be noted that there are important differences between the present experimental conditions and previous electronic structure calculations. First, theoretical calculations were carried for the 1:1 stoichiometric Li-Cs alloy. Second, the effect of temperature was not considered. As demonstrated here, a thermal activation is required to obtain the cubic crystalline alloy. Again, these two factors were not considered in the calculations. Perhaps the most significant observation arising from the present work is that the experimental charge density unambiguously shows that charge donation from Cs to Li is feasible at low pressure in which Li uses the diffuse  $2p$  orbitals to accommodate the electron and adopt a formal oxidation state of  $-1$ . Although first-principles structural prediction techniques (21–23) are known as a powerful complement to experiments, our study indicates that the prediction of structures for nonstoichiometric alloys still represents a significant challenge. Together with recent theoretical studies (3, 4), the present experimental findings illustrate the diversity of chemical bonding manifested by the apparently simple group I elements.

## MATERIALS AND METHODS

High-purity Li and Cs metals (Alfa Aesar, 99.999%) were loaded and constrained, under an inert argon atmosphere, by a rhenium gasket placed between anvils presenting 350- $\mu\text{m}$ -diameter culets of resistively heated membrane DACs. Because Li and Cs are very reactive under normal laboratory conditions, the sample purity was confirmed by x-ray diffraction after the DAC loadings; no trace of the metal oxides or hydroxides was found. Powder x-ray diffraction images were recorded on a Rigaku R-axis IV++ area detector at beamline BL10XU of SPring-8 (Japan) using x-rays with a wavelength of 0.41373 Å from samples at different pressures ( $T < 10$  GPa) and temperatures ( $T < 500$  K). The x-ray beam was focused at the sample using a compound refractive lens (24). Temperature was measured using thermocouples placed inside the DAC, on the gasket, and the quasi-hydrostatic pressures were obtained from the calibrated spectral shifts of ruby luminescence corrected at each temperature. X-ray diffraction images were integrated using FIT2D (25), and the resulting x-ray diffraction patterns were analyzed using XRDA software (26); full pattern refinements were carried out by the Rietveld method using the FULLPROF software (27). To perform the MEM analysis, the intensities of the Bragg peaks were extracted using the Le Bail method (28). The charge density was then derived from the MEM program PRIMA (29). The MEM calculations were initiated from a uniform prior density distribution, resulting from dividing the total number of electrons in the unit cell. All MEM calculations were performed over a  $64 \times 64 \times 64$  pixel mesh representing the unit cell.

## REFERENCES AND NOTES

1. A. R. Miedema, P. F. de Châtel, F. R. de Boer, Cohesion in alloys—Fundamentals of a semi-empirical model. *Physica B* **100**, 1–28 (1980).
2. W. J. Hume-Rothery, in *Series in Material Science and Engineering*, P. S. Rudman, J. Stringer, T. Jaffee, Eds. (McGraw-Hill, New York, 1967), chap. 3.
3. X. Zhang, A. Zunger, Altered reactivity and the emergence of ionic metal ordered structures in Li-Cs at high pressures. *Phys. Rev. Lett.* **104**, 245501 (2010).
4. J. Botana, M.-S. Miao, Pressure-stabilized lithium caesides with cesium anions beyond the  $-1$  state. *Nat. Commun.* **5**, 4861 (2014).
5. T. Atou, M. Hasegawa, L. J. Parker, J. V. Badding, Unusual chemical behavior for potassium under pressure: Potassium–silver compounds. *J. Am. Chem. Soc.* **118**, 12104–12108 (1996).
6. J. S. Tse, G. Frapper, A. Ker, R. Rousseau, D. D. Klug, Phase stability and electronic structure of K-Ag intermetallics at high pressure. *Phys. Rev. Lett.* **82**, 4472–4475 (1999).
7. J. S. Tse, S. Desgreniers, Y. Ohishi, T. Matsuoka, Large amplitude fluxional behaviour of elemental calcium under high pressure. *Sci. Rep.* **2**, 372 (2012).
8. M. Sakata, M. Takata, The principle of the maximum entropy method. *High Press. Res.* **14**, 327–333 (1996).
9. J. S. Tse, R. Flacau, S. Desgreniers, J. Z. Jiang, Electron density topology of high-pressure  $\text{Ba}_8\text{Si}_{46}$  from a combined Rietveld and maximum-entropy analysis. *Phys. Rev. B* **76**, 174109 (2007).
10. J. S. Tse, M. Hanfland, R. Flacau, S. Desgreniers, Z. Li, K. Mende, K. Gilmore, A. Nyrow, M. M. Sala, C. Sternemann, Pressure-induced changes on the electronic structure and electron topology in the direct FCC→SH transformation of silicon. *J. Phys. Chem. C* **118**, 1161–1166 (2014).
11. T. Noritake, M. Aoki, S.-i. Towata, Y. Seno, Y. Hirose, Charge density analysis of magnesium hydride. *R&D Rev. Toyota CRDL* **38**, 15–21 (2003).
12. P. W. Bridgman, Rough compressibilities of fourteen substances to 45,000 kg/cm<sup>2</sup>. *Proc. Am. Acad. Arts Sci.* **72**, 207–225 (1938).
13. P. W. Bridgman, The compression of 39 substances to 100,000 kg/cm<sup>2</sup>. *Proc. Am. Acad. Arts Sci.* **76**, 55–70 (1948).
14. M. S. Anderson, C. A. Swenson, Experimental equations of state for cesium and lithium metals to 20 kbar and the high-pressure behavior of the alkali metals. *Phys. Rev. B Condens. Matter* **31**, 668–680 (1985).
15. H. T. Hall, L. Merrill, J. D. Barnett, High pressure polymorphism in cesium. *Science* **146**, 1297–1299 (1964).
16. K. Takemura, S. Minomura, O. Shimomura, X-ray diffraction study of electronic transitions in cesium under high pressure. *Phys. Rev. Lett.* **49**, 1772–1775 (1982).
17. M. I. McMahon, R. J. Nelmes, S. Rekh, Complex crystal structure of cesium-III. *Phys. Rev. Lett.* **87**, 255502 (2001).
18. R. M. Sternheimer, On the compressibility of metallic cesium. *Phys. Rev.* **75**, 888–889 (1949).
19. C. E. Weir, G. J. Piermarini, Lattice parameters and lattice energies of high-pressure polymorphs of some alkali halides. *J. Res. Nat. Bur. Stand.* **68A**, 105–111 (1964).
20. [https://en.m.wikipedia.org/wiki/Ionic\\_radius](https://en.m.wikipedia.org/wiki/Ionic_radius)
21. A. R. Oganov, Ed., *Modern Methods of Crystal Structure Prediction* (Wiley-VCH, Berlin, 2010).
22. C. J. Pickard, R. J. Needs, *Ab initio* random structure searching. *J. Phys. Condens. Matter* **23**, 053201 (2011).
23. Y. Wang, J. Lv, L. Zhu, Y. Ma, Crystal structure prediction via particle-swarm optimization. *Phys. Rev. B* **82**, 094116 (2010).
24. Y. Ohishi, N. Hirao, N. Sata, K. Hirose, M. Takata, Highly intense monochromatic X-ray diffraction facility for high-pressure research at SPring-8. *High Press. Res.* **28**, 163–173 (2008).
25. A. P. Hammersley, S. O. Svensson, M. Hanfland, A. N. Fitch, D. Häusermann, Two-dimensional detector software: From real detector to idealised image or two-theta scan. *High Press. Res.* **14**, 235–248 (1996).
26. S. Desgreniers, K. Lagarec, *XRDA*: A program for energy-dispersive X-ray diffraction analysis on a PC. *J. Appl. Crystallogr.* **27**, 432–434 (1994).
27. J. Rodriguez-Cavajal, Recent developments of the program FULLPROF. *Comm. Powder Diffract. Newsl.* **26**, 12–19 (2001).
28. A. Le Bail, Modelling anisotropic crystallite size/microstrain in Rietveld analysis. *NIST Spec. Publ.* **846**, 142–153 (1992).
29. F. Izumi, R. A. Dilanian, *Recent Research Developments in Physics* (Transworld Research Network, Trivandrum, India, 2002), vol. 3, pp. 699–726.
30. B. Olinger, J. W. Shaner, Lithium, compression and high-pressure structure. *Science* **219**, 1071–1072 (1983).

**Acknowledgments:** We thank the Japan Synchrotron Radiation Research Institute (JASRI) for beam time and the Government of Canada for Tier I Canada Research Chair to J.S.T. **Funding:** Support from NSERC of Canada and the Canada Foundation for Innovation is acknowledged. **Author contributions:** S.D. and J.S.T. designed the experiment. Y.O. and T.M. designed and built the necessary instrumentation at SPring-8 (Japan) to carry out the experiments and prepared the samples. All authors participated in the experiments. S.D. and J.S.T. analyzed the data and wrote the initial manuscript. All authors contributed to the final manuscript. **Competing interests:** The authors declare that they have no competing interests. **Data and materials availability:** Data is available upon request to the corresponding authors.

Submitted 25 May 2015  
 Accepted 17 August 2015  
 Published 9 October 2015  
 10.1126/sciadv.1500669

**Citation:** S. Desgreniers, J. S. Tse, T. Matsuoka, Y. Ohishi, J. J. Tse, Mixing unmixables: Unexpected formation of Li-Cs alloys at low pressure. *Sci. Adv.* **1**, e1500669 (2015).